Cathode Materials

Surface Modification Strategies for Improving the Cycling Performance of Ni-Rich Cathode Materials

Daniel Weber,[a][‡] Đorđije Tripković,[a][‡] Katja Kretschmer,[a][‡] Matteo Bianchini,[a,b] and Torsten Brezesinski*[a]

Abstract: Ni-rich layered lithium metal oxides are the cathode active materials of choice for high-energy-density Li-ion batteries. While the high content of Ni is responsible for the excellent capacity, it is also the source of interfacial instability, limiting the material's lifetime due to a variety of correlated in- and extrinsic factors. Hence, reconciling the opposing trends of high Ni content and long-term cycling stability by modifying the material's surface is one of the challenges in the field. Here, we review various studies on surface modification of Ni-rich ($\geq$ 80 %) layered cathode active materials in order to categorize current research efforts. Broadly, the three strategies of coating, surface doping and washing are discussed, each with their advantages and shortcomings. In conclusion, we highlight new directions of research that could bring Ni-rich layered lithium metal oxide cathodes from the laboratory to the real world.

1. Introduction

Lightweight Li-ion batteries (LIBs) are the bedrock of mobile energy-storage systems for high energy and power densities. Especially the layered cathode active materials (CAMs) $LiNi_{1-x-y}Co_xMn_yO_2$ (NCM) and $LiNi_{1-x-z}Co_xAl_zO_2$ (NCA) with $\geq$ 80 % Ni are at the frontier of battery research due to the low content of costly Co, large specific capacity based on Ni redox and the ensuing interest of the automotive sector.[1,2] The goal is to push the specific capacity of layered NCM and NCA to the physical limit represented by $LiNiO_2$ (LNO), with its theoretical specific capacity of 275 mAh/g, while retaining high cycling stability (i.e., end of life after > 1000 cycles). In practice, the current record for the initial specific discharge capacity is at 245 mAh/g in LNO. However, as the material with the highest Ni content compared to other NCM or NCA CAMs, LNO exemplifies problems typical of Ni-rich materials, such as the large (ca. 31 %) capacity loss within the first 100 cycles.[3] This loss is especially aggravating, as a current battery waste management analysis singles out prevention of degradation as a superior strategy vs. second use or recycling.[4]

In CAMs, observed capacity losses originate from extrinsic factors, such as transition-metal dissolution or decomposition of surface carbonates, as well as intrinsic loss mechanisms. The latter are based on changes in chemical bonding between the oxygen and the transition metal upon (de)lithiation, which destabilize the material via various degradation mechanisms, such as oxygen release at the surface and structural phase transitions, leading to mechanical fading.[1,5–8] Especially in Ni-rich materials, the Ni 3d and O 2p states are hybridized, which has been probed directly by various X-ray spectroscopic experiments sensitive to the oxidation state of the constituents.[6,9] Once the Fermi level is lowered by delithiation, the hybridized bands become depopulated, leaving holes on the cation and in case of high voltages also oxidize the oxide anion. This negatively affects the CAM in several ways: first, the changes in chemical bonding result in strong microscopic lattice deformations and large macroscopic volume changes.[10–17] In the example of NCM811 (80 % Ni), the relative variation in unit cell volume is approximately –5 % (at x(Li) $\approx$ 0.2) upon charging to 4.3 V vs. Li$^+$/Li. Another important factor is the weakening of the M–O bond upon delithiation, which leads to oxygen release at the surface and simultaneous formation of a rock salt-type surface layer of low ionic conductivity.[18,19] Concurrently to the release of oxygen, the electrolyte can be oxidized via the reaction with evolved $^1O_2$ species.[20–24] These mechanisms apply both to liquid carbonate electrolytes, which evolve CO and CO_2, and sulfur-based solid electrolytes (lithium thiophosphates), which oxidize to SO_2. Additional capacity losses from factors extrinsic to the CAM are induced by alkaline surface contaminations, such as Li_2CO_3 or transition-metal carbonates, which result from post-synthetic reactant residues and/or suboptimal storage conditions and lead to CO_2 evolution.[25–29] During as-

[a] Dr. D. Weber, Dr. Đ. Tripković, Dr. K. Kretschmer, Dr. M. Bianchini, Dr. T. Brezesinski
    Battery and Electrochemistry Laboratory (BELLA), Institute of Nanotechnology, Karlsruhe Institute of Technology (KIT), Hermann-von-Helmholtz Platz 1, 76344 Eggenstein-Leopoldshafen, Germany
    E-mail: torsten.brezesinski@kit.edu
[b] Dr. M. Bianchini
    BASF SE, Carl-Bosch-Strasse 38, 67056 Ludwigshafen, Germany
[‡] These authors contributed equally to this work.
    ORCID(s) from the author(s) for this article is/are available on the WWW under https://doi.org/10.1002/ejic.202000408.

EurJIC
European Journal of Inorganic Chemistry

Minireview
doi.org/10.1002/ejic.202000408

Chemistry Europe
European Chemical
Societies Publishing

sembly and operation of a battery, additional contaminants, such as HF, may be introduced, which contributes to cation dissolution at high voltages and also leads to anode capacity losses.[30,31] Hence, capacity degradation stems from various facets of changes in the electronic structure as well as extrinsic factors, such as surface impurities, making modification of the surface the key strategy for enhancing the longevity of Ni-rich NCM and NCA CAMs.

The three main strategies for stabilization are the surface modifications by (I) coating, (II) doping and (III) washing for the removal of surface contaminants. Coatings create a physical barrier layer encapsulating the secondary particle and thus supposedly stabilize the CAM by kinetically impeding oxygen evolution and shielding it from interaction with external reactants, such as HF.[18,32,33] Doping, on the other hand, stabilizes the crystal and electronic structure by increasing the thermodynamic or kinetic barrier for oxygen loss and the subsequent progress of the layered to rock salt-type phase transition.[18,34,35]

Introduction of selected dopants either in the last stage of the precipitation or by post-synthetic treatment of the metal hydroxide reactant allows to confine their concentration at the surface. The last main strategy is washing of the CAM in polar solvents to remove detrimental carbonate and/or alkaline surface impurities. The effect of these three strategies are sketched out in Figure 1. They have found wide-spread applications in CAMs, yet in Ni-rich materials, the stabilization via surface modification is crucial because of increased reactivity compared to low-Ni materials.[32,36]

Currently, the need for increasing capacity (energy density) leads to the usage of CAMs with ≥ 80 % Ni, thereby setting limits on future applications of doping and elemental gradient-based strategies within the bulk crystal structure. Consequently, the importance of controlling the cathode-electrolyte interface via surface modification strategies will grow in the future. In this minireview, we summarize current approaches to surface modification to address the stability and longevity issues of the

Daniel Weber studied Chemistry at the Ludwig-Maximilians-University of Munich. During his PhD with Prof. Lotsch at the Max-Planck-Institute for Solid State Research (graduation 2017), he investigated the synthesis of new single-layer materials containing Ru and Ir. He spent two years at the lab of Prof. Goldberger at the OSU (USA) as a postdoctoral fellow, where he worked on layered ferromagnets. Currently, he is a postdoctoral researcher investigating the synthesis and modification of cathode active materials at BELLA.

Đorđije Tripković obtained his PhD in Solid State Electrochemistry from the Technical University of Denmark under the supervision of Prof. Hendriksen and Prof. Mogensen. Since 2019, he is a postdoctoral fellow at BELLA. His research focuses on operando gassing analysis, surface characterization and data-driven investigation of degradation phenomena in LIBs.

Katja Kretschmer obtained her Diplom in Chemical Engineering from TU Braunschweig in 2013 under the supervision of Prof. Krewer. Katja then joined the Centre for Clean Energy Technology (UTS) under the guidance of Prof. Wang to pursue a PhD focusing on polyanionic phosphate-based cathode materials for LIBs and NIBs. Since 2018, she is a postdoctoral fellow at BELLA and her work involves multi-element surface modification of Ni-rich cathode active materials and their long-term stability in LIBs.

Matteo Bianchini studied Physics Engineering at Politecnico di Milano. He obtained his PhD in 2015 with Prof. Masquelier (LRCS, Amiens), Dr. Croguennec (ICMCB, Bordeaux) and Dr. Suard (ILL, Grenoble) for operando diffraction studies on battery materials. He was a postdoctoral researcher for two years in the group of Prof. Ceder at Lawrence Berkeley National Lab, where he worked on the design, synthesis and characterization of new electrode materials. Afterwards, he was a postdoctoral fellow at BELLA investigating Ni-rich cathode active materials for LIBs. He then joined BASF and is currently lab team leader for BELLA.

Torsten Brezesinski obtained his PhD in Physical Chemistry from MPI of Colloids and Interfaces/University of Potsdam in 2005. After years spent at UCLA (USA), he joined the faculty of the Department of Biology and Chemistry at JLU Giessen as an independent group leader in 2008. Since May 2012, he is laboratory manager of BELLA and group leader at the Institute of Nanotechnology of KIT. His research focuses on materials chemistry and electrochemical energy storage.

EurJIC
European Journal of Inorganic Chemistry

Minireview
doi.org/10.1002/ejic.202000408

Chemistry Europe
European Chemical
Societies Publishing
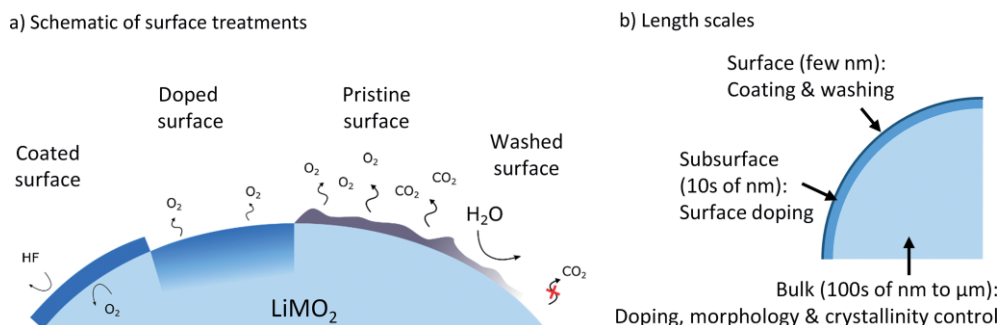
Figure 1. (a) Representation of different modification strategies and their effect on cathode active materials of the formula $LiMO_2$, which contain Ni, Co and Mn or Al, with O_2 and CO_2 evolution as well as HF attack. (b) Effective length scales of various modifications.

Ni-rich NCM surface, in order to complement prior reviews on the topic of CAMs[8,37–41] and to categorize current investigations.

2. Coatings

The fact that almost all degradation mechanisms are related or initiated by surface phenomena has prompted wide research in the application of protective coatings. There are various rationales for using coatings based on which degradation mechanism(s) they are aimed to alleviate. Hence, one way of classifying the multitude of already investigated coatings is by their intended purpose. We discuss the use of coatings as physical barriers, HF shields and HF scavengers along with some other capabilities in section 2.1. This approach may be obscured by the fact that some coatings have multiple effects or that their working principle is not well understood. The functionality of coatings is closely connected to their chemical composition, which is another convenient way of classifying coatings in section 2.2. Finally, applicability and economic viability are inextricably related to processing and coating methodologies, which we discuss in section 2.3.

2.1. Purpose

Physical Barrier

The simplest case is the use of coatings to act as a physical barrier, thereby preventing direct contact between the CAM and the electrolyte. It is well established that during the electrochemical cycling the organic electrolyte can get oxidized and decomposed on the surface, forming a cathode solid electrolyte interphase (cSEI) layer.[42–45] As opposed to the relatively thick and beneficial SEI that stabilizes graphite anodes, cSEI is typically only several nanometers thick, harms cell kinetics and increases impedance. Furthermore, decomposition of electrolyte is accompanied by gassing, which causes safety problems. Coating the material with a passive barrier layer is expected to slow down or eliminate cSEI formation and gassing by thwarting the oxidation of electrolyte on highly reactive centers, such as Ni^{4+}. Such an approach has been demonstrated by Becker et al.,[46]

where residual Li compounds on the surface of NCM811 were transformed into a tungsten oxide-based coating (Li_2WO_4 or WO_3) via a sol-gel route. The authors accredited the remarkable improvement in electrochemical performance (cycle life extended from 465 to 865 cycles) to a uniform layer, acting as a protective shield. Similar reasoning and coating procedures were employed for other compositions. Notable examples include Li_4SiO_4[47] (capacity retention of $LiNi_{0.80}Co_{0.15}Al_{0.05}O_2$ improved from 65.27 % to 88.08 % after 100 cycles at 1C rate without hindering rate capability), $Li_4Ti_5O_{12}$[48] (capacity retention of NCM811 improved from 39.40 % to 75.86 % after 170 cycles at 1C rate) and Li_2ZrO_3[49] (capacity retention of $LiNi_{0.80}Co_{0.15}Al_{0.05}O_2$ in solid-state battery cells improved from 73.9 % to 91.7 % after 100 cycles at C/10 rate).

Despite promising reports and simplicity, the use of coatings as a physical barrier is not without challenges. Since the purpose of coatings is to extend the cycle life by preventing structural changes and increase in internal resistance, it is of paramount significance that the coatings themselves do not contribute to these adverse effects. However, the physical barrier coatings generally increase the cell impedance by hampering lithium diffusion and reduce specific capacity by introducing (electrochemically) inactive material.

Another rarely discussed point of crucial importance for the effectiveness of physical barrier coatings is their morphology and the extent of coverage (see section 2.3). Studies are typically supplemented with TEM images, which can only give local information, and/or SEM, which gives a better overview, but is insufficient for resolving small imperfections in coatings. Even though these methodological problems are common to all types of coatings, this piece of information is crucial for physical barrier coatings, as they assume near perfect and full surface coverage to be effective.

Finally, the very logic behind the use of physical barrier coatings for Ni-rich CAMs is debatable. Firstly CAMs, unlike most coatings, change their volume significantly during cycling, thus continuously opening new unprotected contact points with the electrolyte. Secondly, it has been shown that in case of Ni-rich CAMs, the electrochemical oxidation of electrolyte is negligible compared to chemical oxidation by oxygen released from the lattice in the common operating voltage window.[44,50] Whereas physical barrier coatings can have a beneficial effect on high-

EurJIC
European Journal of Inorganic Chemistry

Minireview
doi.org/10.1002/ejic.202000408

Chemistry
Europe
European Chemical
Societies Publishing

voltage spinel electrodes, such as $LiNi_{0.5}Mn_{1.5}O_4$ (LNMO), their scope of action in Ni-rich CAMs is rather limited and may revolve around disrupting continuous cSEI formation. Another explanation could be that the inactive layer on top of the CAM acts as a retardant of lattice oxygen evolution by providing a kinetic barrier to oxygen migration.[18] Alternatively, the observed beneficial effects of this type of coatings may be largely due to other mechanisms, such as HF protection, discussed in the following section.

HF Protection

In addition to stability issues caused by the intrinsic properties of CAMs, their surface is a target of extrinsic degradation effects. Such is the case of widely reported corrosion by HF, which forms as a product of hydrolysis of the supporting salt $LiPF_6$. This process is practically unavoidable due to traces of water present in the electrolyte, electrodes or cell parts. The emergence of HF in the cell is particularly detrimental not only as a result of its strong leaching effect, but also because it initiates a vicious circle, where water molecules are continuously created in a reaction between the HF and the oxide CAM (Figure 2a).[51] A variety of different materials have been used to protect the surface from HF attack. They can be roughly sorted into two categories: HF scavengers and HF barriers.

Scavengers are compounds that have a high affinity towards HF.[52,53] The idea is to sacrifice the scavenger material in reaction with HF, thereby reducing the amount reacting with the surface of the CAM. Because of the nature of the protective mechanism, HF scavenger coatings do not require uniform and tight coverage, which can largely simplify the coating procedure (see schematic representation of coating morphologies in Figure 2b-d). The effect of scavenger coatings is expected to be higher for a large surface-to-volume ratio (e.g., nanoparticulate coatings), as the scavenger should ideally have a much larger specific surface area than the CAM. Via reaction between the HF and the scavenger, however, the same vicious circle of H_2O generation and HF formation is initiated as when HF reacts with the unprotected surface. This eventually leads to conversion of the whole scavenger mass to respective fluorides, which may (to some degree) only physically protect the surface while hindering lithium diffusion. Hence, the obvious disadvantage of scavenger coatings is the limited time of the effect. In other words, scavenger coatings only postpone the inevitable degradation, which depends on the initial amount of moisture in the cell. Typical examples include binary oxides, such as Al_2O_3.[54–56] For example, by coating the surface of $LiNi_{0.8}Co_{0.15}Al_{0.05}O_2$ with a nanoparticulate Al_2O_3 layer, Du et al.[54] reported a remarkable improvement in cycling performance at 1C rate and different temperatures and cutoff voltages. The improvement was shown to be even higher for harsher cycling conditions (4.5 V, 55 °C) when electrolyte decomposition is expected to be more pronounced (discharge capacity retention improved from 59.47 % to 81.1 % after 150 cycles).

HF barriers, as opposed to scavengers, assume low reactivity and good electrochemical and thermodynamic stability. These coatings require uniform and pinhole-free coverage to be effective. However, this leads to a higher impedance and lower lithium diffusivity, since HF barriers are generally poor ionic and electronic conductors.

Apart from the complicated task of obtaining continuous coating, another problem with barrier coatings may appear during prolonged electrochemical cycling. As the size of cathode particles changes during (de)lithiation, pressure on the barrier coating increases, eventually leading to fracturing. The amount of HF present in the system does not change and is readily available to attack any surface exposed by cracks in the coating and initiate the H_2O-HF cycle. Materials used for this purpose include binary oxide coatings (e.g., WO_3[57]), phosphates (e.g., $LiMnPO_4$[58]) and glasses (Li_2O-B_2O_3[59]), to name a few. Promising results were obtained by Jang et al.[60] using barrier coating with HF scavenging groups. This combined approach involved coating NCM811 with a 5 nm layer of lithium tetra(trimethylsilyl) borate, which resulted in improved capacity retention from 54.4 % to 75 % after 100 cycles at C/10 rate and 55 °C. The silylborate functional group (Si–O–B) acted as HF scavenger while intimate contact with the CAM was achieved via bond between B and O from the layered structure.

An alternative approach has been demonstrated by Rodrigues et al.[61] and consists in removal of moisture from the system in the first place by using hygroscopic agents, such as MgO nanoparticles. In the aforementioned study, the nanoparticles served as electrolyte additives; however, the use of hygroscopic coatings has not yet been thoroughly investigated. Furthermore, in a computational study, Aykol et al.[53] summarized
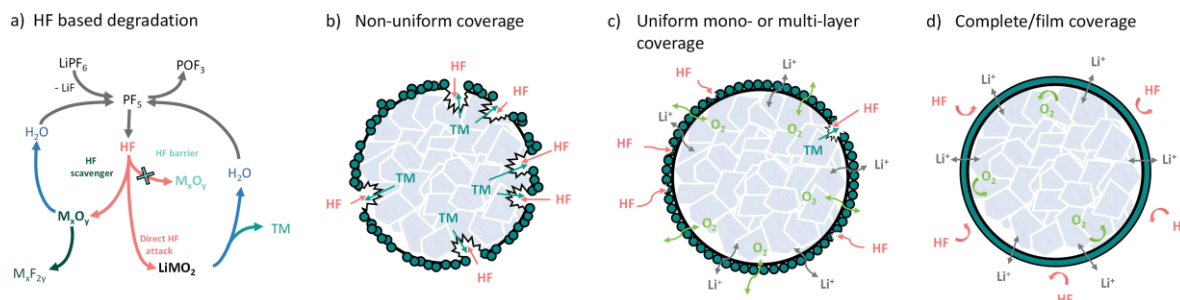
Figure 2. (a) Mechanistic and schematic representation of HF (re)generation and possible protection strategies. Pink arrows indicate paths of HF towards the surface. Blue arrows illustrate regeneration of water in the system. TM stands for transition metal. Note that in each scenario the overall amount of HF remains constant. (b-d) Schematic representation of coating morphologies, their potential resistance to HF attack and possible Li+ and O_2 pathways. The shape of the arrows indicates reaction/transport kinetics (straight: fast, s-shape: hindered, curved: blocked). (b) Non-uniform nanoparticulate coverage. (c) Uniform mono- or multi-layer coverage (particulate or sheet-like). (d) Complete/film coverage (core-shell or thin film).

EurJIC
European Journal of Inorganic Chemistry

Minireview
doi.org/10.1002/ejic.202000408

Chemistry Europe
European Chemical Societies Publishing

promising candidates for both HF barrier and scavenging purposes, many of which have not yet been tested experimentally, thus leaving room for further improvements in preventing HF-induced degradation.

Other Purposes

Apart from the main mechanisms discussed above, the coatings often exhibit additional beneficial effects. Residual lithium compounds (see section 4) have an adverse effect on the electrochemical performance because of their intrinsically low ionic conductivity and subsequent decomposition accompanied by gassing. Some coatings can convert these residuals into reasonably conductive lithium compounds, such as phosphates[62,63] and garnets,[64] thereby improving the rate capability. It has been claimed that polymeric coatings, which generally achieve full surface coverage more readily, can prevent cracking by giving elastic support to the secondary particles.[65,66] Other reported beneficial effects of coatings include suppression of transition-metal dissolution[67] and improved thermal stability.[68,69] The latter is especially important for safety of the battery during operation. The prevention of structural disarrangement in the outer surface layers is often claimed as the result of coatings. This effect is usually connected with the migration of ions from the coating to the CAM surface at elevated temperatures, i.e., surface doping (see section 3).

2.2. Composition

Coatings are also frequently classified by composition. This can be done either by cation or anion. In the following, we will use anion-based classification to list some of the most frequently used types of coatings, namely oxides, phosphates and fluorides. We also discuss some interesting coatings that do not fall into these classes, such as polymer coatings and organometallic modifications.

Oxides

The idea behind the use of oxide coatings is usually to establish a chemically stable protective layer to shield the surface from adverse side reactions with the electrolyte. The strong covalent bond present in oxides ensures this function. However, low electronic and ionic conductivity often lead to high impedance and poor kinetics. These problems can, to some extent, be resolved by calcination and reaction with Li compounds, typically present at the surface of Ni-rich CAMs. The resulting mixed Li-containing oxides are better ion conductors and often retain the same stability as the starting oxides. Furthermore, oxide coatings can act both as HF barrier and scavenger.[53] Typical examples include Al_2O_3,[54,68,70–72] TiO_2[68,73,74] and ZrO_2.[49,75] Oxide coatings based on tungsten,[57] boron,[59] cobalt,[76] silicon[68] and tin[77] have also been reported. Usually, these studies examine single oxide coatings and compare the performance with the bare material. However, there are also comparative studies of different coatings. Such is the study of Hildebrand et al.,[68] where the effect of SiO_2, Al_2O_3 and TiO_2 coating on the thermal stability of $LiNi_{0.8}Co_{0.15}Al_{0.05}O_2$ was assessed, showing the most promising results for the SiO_2 coating.

Phosphates

The function of phosphate-based coatings is usually closely connected to residual Li compounds that are present on the surface of Ni-rich CAMs. Treatment with phosphates can be used to convert lithium hydroxides and carbonates, being electrochemically inert and detrimental for long-term cycling stability, into an active and ionically conducting layer that can provide further surface protection.

This approach is well demonstrated by Xiong et al.[78] The authors used $(NH_4)_2HPO_4$ to treat the surface of NCM811, anticipating the reaction with Li hydroxides and formation of a Li_3PO_4 coating layer. Their results show that this is an effective way to passivate the surface hydroxides and prevent the propagation of the H_2O-HF cycle; yet, continuous surface coating could not be achieved. Focusing on obtaining full particle coverage, Tang et al.[79] first enriched the cathode surface with phosphate anions and subsequently lithiated with Li_2CO_3. The obtained Li_3PO_4 coating was then shown to be an effective shield, capable of preventing side reactions between the cathode and the electrolyte. However, Li_3PO_4 is electronically insulating. To overcome this, Chen et al.[65] combined Li_3PO_4 with the electronically conductive polymer polypyrrole (PPy), thereby achieving good surface coverage without significantly increasing impedance.

Other phosphates of olivine crystal structure, containing mostly transition metals, have been studied based on their exceptional thermal and chemical stability and good Li-ion conductivity.[58,62,69,80,81] In a comprehensive study by Min et al.,[82] 16 different metal phosphate coatings were computationally screened for their ability to remove residual Li species (Li_2O) and form stable olivines. Four candidates ($Mn_3(PO_4)_2$, $Co_3(PO_4)_2$, $Fe_3(PO_4)_2$ and $TiPO_4$) were also experimentally tested, showing that all of them, except $TiPO_4$, resulted in improved capacity retention (Figure 3). However, only $Co_3(PO_4)_2$ was able to increase the stability without compromising the initial specific capacity of NCM910603 (91 % Ni). These findings well illustrate both the potential (chemical stabilization) and the disadvantage (poor conductivity) of phosphate-based coatings, suggesting that further improvements may be achieved by tailoring the coating amount and morphology.

Fluorides

Fluoride coatings have often been applied to serve as thermodynamically stable barriers between the cathode and the electrolyte. Fluoride coatings are typically obtained by mixing ammonium fluorides and respective metal nitrates,[83–85] but some have been deposited by atomic layer deposition (ALD).[86] The tested compositions include AlF_3,[83,84] $LiAlF_4$,[86] FeF_3[87] and LiF.[85] Surface modification with LiF is expected to shift the equilibrium of electrolyte decomposition reaction ($LiPF_6 \rightleftharpoons LiF + PF_5$) to the left, thereby preventing HF formation in the system.[85] In addition to improved capacity retention, the study also shows better rate capability for the material covered with LiF. This finding is curious considering that the same authors attributed the beneficial effect of $(NH_4)_2HPO_4$ treatment to the removal of detrimental LiF from the surface, which is a poor Li-ion conductor. In an endeavor to simultaneously improve the

EurJIC
European Journal of Inorganic Chemistry

Minireview
doi.org/10.1002/ejic.202000408

Chemistry Europe
European Chemical
Societies Publishing
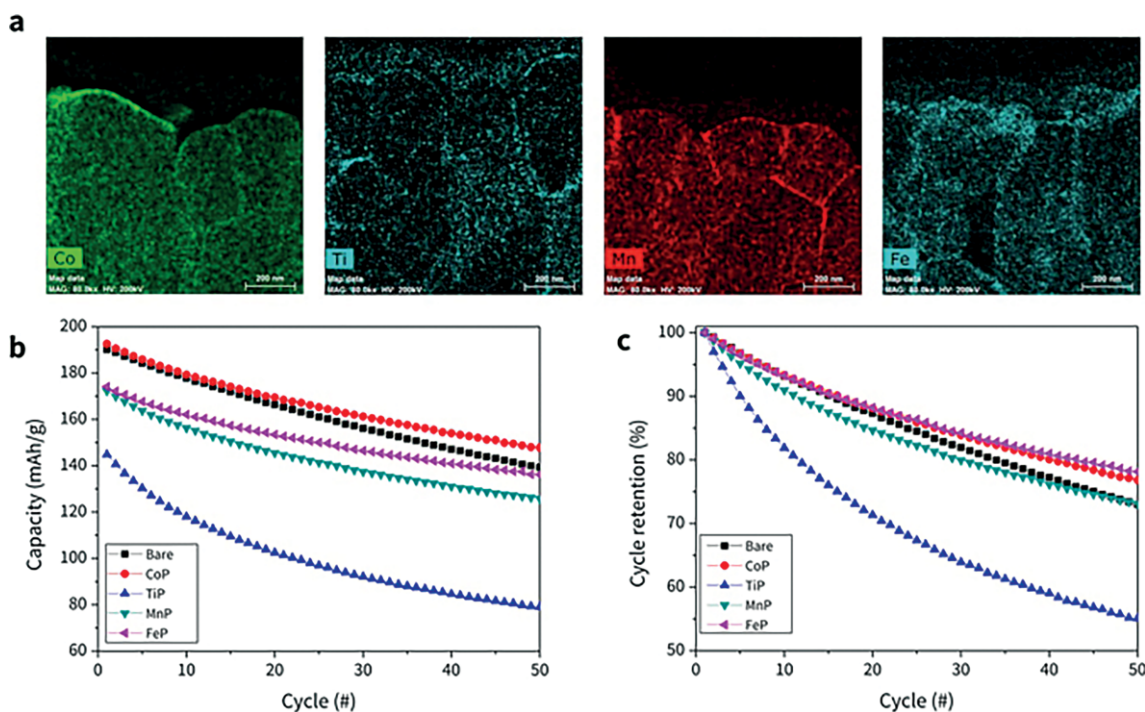
Figure 3. (a) EDS elemental mapping of $Mn_3(PO_4)_2$-, $Co_3(PO_4)_2$-, $Fe_3(PO_4)_2$- and $TiPO_4$-coated NCM910603 (denoted as MnP, CoP, FeP and TiP). (b) Specific capacity at 1C rate and (c) the respective capacity retention. Reproduced from ref.[82]

surface coverage and ionic conductivity, Xie and co-workers coated the surface of NCM811 with $LiAlF_4$, a thermodynamically stable compound.[86] The authors have shown that in comparison with bare material, $LiAlF_4$ coating leads to improved Coulombic efficiency, rate capability and capacity retention, while the opposite is observed for LiF and AlF_3 coatings, which was rationalized by the four order of magnitude higher Li-ion conductivity of $LiAlF_4$.

Despite the promising reports on fluoride coatings, we must conclude that, based on the current reports, their effect is still not fully understood, which leaves room for further enhancements.

Composites

There is an overall impression that the majority of coating studies are done in an almost random fashion. Different cations are implemented in the form of oxides, phosphates and fluorides, usually showing an improvement when compared to bare material. However, the mechanistic aspects of proposed explanations of improvements are rarely supplemented with hard proofs. As opposed to this approach, there is an ongoing trend in the community towards highly engineered composite coatings. These coatings combine functionalities of different materials or active centers to tackle a specific task. Frequently, such coatings entail polymer-based or organometallic parts, which exploit the malleability of organics to achieve full surface coverage and give additional mechanical support to the secondary particles.

A good example is the study by Gan et al.,[66] where a conducting polymer coating was employed to improve the electro-
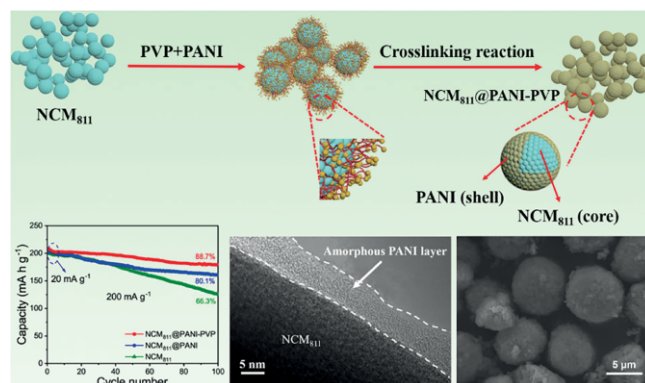
Figure 4. Schematic illustration of the preparation of NCM811@PANI–PVP (top) as well as plot of the cycling performance data and cross-sectional TEM and top-view SEM images of the coated surface and secondary particles, respectively (bottom). Reproduced with permission from ref.[66] Copyright (2019) American Chemical Society.

chemical cycling stability of NCM811 (Figure 4). The polymer is a composite of polyvinylpyrrolidone (PVP), which binds to the NCM surface, and very stable and electronically conductive polyaniline (PANI). This way, one can achieve optimal and robust surface coverage, which gives mechanical support to particles against fracturing and ultimately improved the electrochemical performance (from 66.3 % to 88.7 % capacity retention after 100 cycles; 20 mA/g and 200 mA/g in the first five and the subsequently cycles, respectively). Another interesting approach was demonstrated by Doo et al.,[88] where the authors applied a 15 nm hydrophobic polydimethylsiloxane coating to NCM811 to prevent the formation of LiOH and Li_2CO_3 on the

EurJIC
European Journal of Inorganic Chemistry

Minireview
doi.org/10.1002/ejic.202000408

Chemistry
Europe
European Chemical
Societies Publishing

particle surface. The coating increased the hydrophobicity of the NCM surface, as shown by contact angle measurements. The hydrophobic NCM featured extended cycle life after storing at 25 °C and 25 % relative humidity for two weeks, indicating the importance of proper material handling and storage for Ni-rich CAMs. To tackle the commonly encountered problem of having either electronic or ionic conductivity, Chen et al. prepared a continuous composite coating consisting of electronically conductive PPy and Li_3PO_4 (providing paths for fast lithium diffusion).[65] The capacity retention after 200 cycles at 1C rate was improved from 65.8 % for bare NCM811 to 86.5 % for coated samples.

Taken together, engineered composite coatings provide a very promising and effective way of addressing common problems during electrochemical cycling; however, their scalability to industrial applications is yet to be tested.

2.3. Preparation Methods

The classification by preparation method attempts to give an overview of available synthetic procedures and their capabilities to generate different coating morphologies and coverage depending on the desired functionality of the applied coating, as discussed in section 2.1. The following section will present techniques, such as wet-chemical methods, ALD as gaseous process (physical deposition) and their combinations.

Sol-Gel

The sol-gel method is well-established to prepare metal oxide particles as well as mixed composites with control over morphology and particle size. It is furthermore a multistep approach that involves hydrolysis, condensation and a drying process, typically resulting in a xerogel or aerogel depending on the drying conditions.[89] In any case, the product generally features some porosity (note that porosity level and specific surface area can be very large, especially for aerogels), with structures in the mesopore (2–50 nm) and/or micropore (≤ 2 nm) size ranges.[90] Hence, the coating morphology achievable using this method can only be described as non-uniform (Figure 2b). However, claims of non-uniform coverage[75] as well as uniform surface films[58] on Ni-rich NCMs have been made. The latter should rather be considered a simplification of the definition of a xerogel, as complete film coverage can hardly be achieved using the sol-gel method. The improved uniformity of the second example is merely a result of the solvent applied in the process, since the sol-gel method can be divided into aqueous and non-aqueous.

The aqueous route applied by Lee et al.[75] provides poor control over particle/coating morphology and was thus described by the authors as non-uniform. Furthermore, it should be noted that using an aqueous system to modify Ni-rich NCMs comes with its very own challenges, such as Li^+ leaching (see section 4). The non-aqueous method applied by Duan et al.[58] is more suitable for the preparation of nanoparticles[89] and the final coating might thus resemble a film-like structure. The relatively uniform coverage also improves the protective effect of this coating, as more reactive surface of the NCM secondary

particle is covered. Becker et al.[46] applied a non-aqueous sol-gel method and particularly evaluated the coating under practical long-term cycling conditions, clearly demonstrating its protective properties. Hence, the non-aqueous sol-gel method, although likely only leading to non-uniform coverage, appears very suitable and somewhat practical for the surface modification of Ni-rich CAMs.

Hydrolysis

Hydrolysis generally describes the cleavage of chemical bonds through the addition of water or a base. The hydroxide ion supplied by either water or base severs a chemical bond and two new bonds are formed, one with the hydrogen and one with the hydroxyl component of water.[91] This approach is used to modify Ni-rich CAMs mostly in its very basic form without any optimization or process parameter variation to control the hydrolysis of the precursor materials.[47,92] Also, the morphology of the resulting coating is not clearly described nor displayed. However, Xiong et al. recently attempted the precise control of reaction kinetics and equilibrium using a buffer solution that keeps precipitation and decomposition rate nearly balanced (Figure 5).[93] In their approach, a coating that can be classified as coverage of around 4 nm was achieved, which was also beneficial for the cycling performance of the CAM. Even though this method appears complex at first glance, a further optimized variant of it might be applicable on a larger scale, even possibly implemented into the already scaled co-precipitation process of precursors prior to lithiation, as was conducted on a $Ni_{0.8}Mn_{0.1}Co_{0.1}(OH)_2$ precursor.
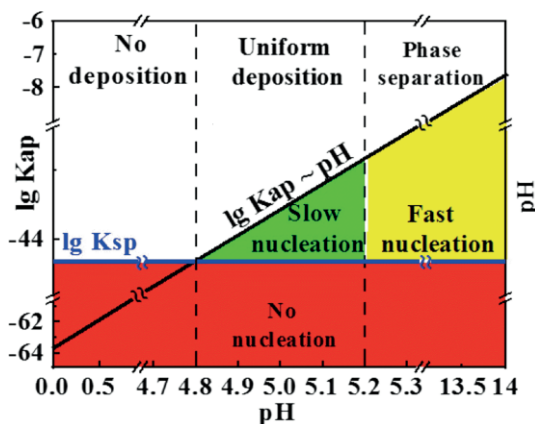
Figure 5. Linear relationship of lg K_{ap} vs. pH value and lg K_{sp} reference line plotted on the graph [K_{ap}: ionic product, K_{sp}: solubility product of the $Ti(OH)_4$]. Note that the coordinate axes are not consecutive or proportional to highlight the critical pH range (4.8–5.2) suitable for uniform coating. Reproduced with permission from ref.[93] Copyright (2019) American Chemical Society.

Precipitation

Co-precipitation is commonly used to synthesize various transition-metal hydroxides and oxides. The mechanism that is being exploited is the solubility difference of salts in aqueous solution. As these water-soluble salts react, one or more salts that are water-insoluble are formed in the liquid phase. Once the concentration of the product passes the solubility product value,

EurJIC
European Journal of Inorganic Chemistry

Minireview
doi.org/10.1002/ejic.202000408

Chemistry Europe
European Chemical
Societies Publishing

precipitation takes place.[94] It is also possible to use this method to form shells/coatings on preformed (core) particles, assuming the product of this reaction precipitates on the core surface rather than in the solution. Because this method is supposed to yield small particles precipitated on the pre-existing larger ones, it is expected to produce a non-uniform coverage, unless the particles can be transformed into a dense shell in a subsequent treatment. As a surface modification method, co-precipitation has been applied to, for example, transform Li impurities on the particle surface into less reactive species, such as LiF,[85] or to introduce a solid electrolyte coverage[64] on NCM. Although this method might not be suitable as a coating strategy, it is very likely to be useful in a potential aqueous slurry preparation process of Ni-rich CAMs, as will be discussed in section 4.

Polymerization/Crosslinking

Polymerization is the process in which monomers, also called building blocks, are chemically bonded under high temperature, pressure or in the presence of a catalyst. This creates larger molecules or macromolecules, which then collectively form a polymer.[95] Chemical crosslinking describes the process of linking these polymer chains to three-dimensional networks, usually resulting in enhancement of mechanical and barrier properties of the structure.[96] Chen et al.[65] applied chemical oxidation polymerization of PPy as electron conductor combined with an ionically conductive Li_3PO_4 coating, which created an overall coverage of over 40 nm. Cao et al.[97] attempted a similar approach using a combination of electronically conducting PANI and ionically conducting PEG, although the polymerization was conducted before introducing the CAM. In both cases, several electrochemical properties could be at least slightly improved. Notably, both studies investigated the effect of their respective coatings on transition-metal dissolution, which is a rare sight. It appears that the application of polymers as surface modification has a significant beneficial effect on preventing transition-metal leaching from the CAM during cycling operation. According to the authors, a "stretchy" and uniform coverage is achieved (Figure 2d as ideal representation) that can withstand cycling-induced stress for some time. Gan et al.[66] also coated a uniform layer of PANI on the surface of Ni-rich NCM via a crosslinking process in the presence of a surfactant (PVP). The improvement in structural stability of the modified CAM was confirmed by XRD and Raman spectroscopy upon (de)lithiation. Conclusively, it can be assumed that the polymerization/crosslinking process holds the most promise out of all wet-chemical routes in achieving a true complete/thin film coverage (Figure 2d). However, because these examples still reported rapid capacity decay, the coatings cannot possibly be complete, and the electrolyte is still able to penetrate them after a short cycling time (ca. 100 cycles are usually shown). Hence, further research is needed to reveal the full potential of this otherwise promising method.

Atomic Layer Deposition

The process of ALD is a gas phase-based technique for the deposition of conformal thin films (mostly metal oxides in case of battery materials) in the range of up to several nanome-

ters.[38,98] Its main characteristic is the self-limitation due to the stepwise reaction of two gaseous species on a surface under low pressures, usually in the sequence of (1) metal precursor, (2) purge gas, (3) H_2O and (4) purge gas. In the first step, the metal precursor adsorbs to the surface and reacts with reactive sites, such as hydroxyl groups, until no further sites are available and residual physisorbed precursor is removed by the purge gas. In the subsequent step, H_2O is injected, leading to the hydrolysis (oxygenation) of metal precursor on the surface until a monolayer of hydroxylated metal species is formed. Residual H_2O is removed by the second purge and the process starts anew. Consequently, film uniformity, conformality and coverage are usually high, as the gaseous reactants can enter easily into crevices and pores, but their reaction with the surface is self-limited due to the sequential nature of the ALD process. This sets ALD apart from chemical bath deposition or line-of-sight techniques, such as physical vapor deposition, which create thicker films on the surface of particles but do not reach into pores and cracks of rough surfaces of the CAM secondary particles. For Ni-rich NCMs and NCAs, the technique has been used to deposit Al_2O_3,[71,99–101] $LiAlO_2$,[102] $LiAlF_4$,[86] Li_3PO_4[103] and TiO_2.[99] However, many of the available ALD coating materials and routes[104] are unexplored to date or have only been tested for low-Ni CAMs.

Currently, several criteria for material choices are debated, such as Lewis acidity, electrochemical stability vs. Li^+/Li or resistance to HF attacks.[105] Another important parameter is whether powder or electrode tape is exposed to the ALD process, as electrical contact to the current collector may be blocked in the former but enabled in the latter case. Fortunately, pilot plants for both procedures have become available in recent years,[38,99,106] making the technique highly relevant for future industrial applications.

Other Methods

Simultaneous coating and drying refers to a coating method developed by Neudeck et al., utilizing the highly H_2O-reactive trimethylaluminum (TMA) commonly utilized in ALD.[72] Diluted TMA reacts with surface adsorbed water, which is an inherent feature in Ni-rich CAMs, according to the following equation: $Al_2(CH_3)_6 + 3H_2O \rightarrow 6CH_4 + Al_2O_3$. Once all water is consumed by this reaction, TMA remains inert in solution and no further precipitation takes place, making the hydrolysis a self-limiting reaction. As a rule of thumb, 500 ppm of adsorbed surface water can be converted into a ca. 1 nm Al_2O_3 coating. Unreacted TMA is simply removed upon solvent evaporation and thus should be supplied in excess to ensure complete elimination of surface water. Adsorbed water is common in industrial settings, where water-based washing procedures are applied for the removal of residual Li species, as described in section 4. Hence, the simultaneous coating and drying method that can be easily controlled by the native moisture of CAM has also great value in large-scale applications. The most remarkable aspect of this coating method in comparison to many others is the significant improvement in cycle life that was achieved. The authors applied it on a commercial NCM811, which extended the cycle life by over 100 % from 500 to 1100 cycles (single-layer pouch full cells cycled at 1C rate and 45 °C). Further analysis on coating

EurJIC
European Journal of Inorganic Chemistry

Minireview
doi.org/10.1002/ejic.202000408

Chemistry Europe
European Chemical
Societies Publishing

morphology as well as optimization (including the screening for other potential precursor candidates) of this method is currently ongoing. However, conclusively it can be said that this combined coating and drying method holds great potential as surface modification strategy for Ni-rich CAMs.[72,107] Many highly reactive metal-organic compounds exist that essentially function in a similar fashion, which may otherwise be difficult to apply as a coating layer. It would also be interesting to explore interactions or synergies between different precursor materials using this strategy or the effect of post-treatment in future studies.

Spray-drying generally describes the transformation of a fluid (solution, suspension, emulsion, slurry, paste or melt) into a powder in hot drying gas. The process consists of atomization of the liquid feed, drying of the resulting spray in the hot gas stream, formation of (dry) particles, their separation from the drying gas and collection. Although well established as large-scale industrial process, parameters that affect the final product are numerous. Flow rates, in- and outlet temperatures, drying gas, feed concentration and solvent properties, to name a few, are all tailorable parameters to modify the final dry product in terms of morphology, particle size, porosity, humidity and so on. Consequently, it is no surprise that this method has not been intensively used in the context of surface modification of Ni-rich CAMs, as it requires a lengthy optimization period. It is rather used for the purpose of synthesizing precursor materials as an alternative to the standard co-precipitation method.[108] Du et al.[54] coated a thick (> 30 nm) layer of Al_2O_3 on a $Ni_{0.80}Co_{0.15}Al_{0.05}(OH)_2$ precursor, which after lithiation at high temperatures transforms into a conducting $LiAlO_2$ coating. The final coating appears conformal due to the unusually large thickness; however, high-resolution TEM imaging clearly reveals the particulate structure of the coverage. Nevertheless, some crucial benefits could be demonstrated, such as improved cycle life (especially at high temperatures) and thermal stability, which can be mainly attributed to the thick and dense coverage. It may be possibly to assume that spray-drying is one of the few methods discussed here that can achieve a somewhat uniform multi-layer coverage, as depicted in Figure 2c. However, more studies of this kind are needed to draw a definite conclusion.

3. Surface Doping

Another important path towards modification of the surface in Ni-rich NCMs is elemental substitution or doping within the first tens of nanometers.[1,3,109,110] Considering length scales, the method modifies the subsurface region. For that reason, it can be distinguished from coatings, which mostly affect the direct particle surface, and bulk doping or transition-metal gradients, which modify several hundreds of nanometers or the complete secondary particle. In a standard process, a coating containing the dopant is applied to the secondary particles, which are then heated to temperatures in the range between ca. 400 °C and 700 °C to induce diffusion of the dopant into the crystallites (primary particles). An alternative approach is the co-precipitation of dopants with a high-temperature miscibility gap during

the hydroxide reactant synthesis. By doing so, the dopant will migrate outwards during heat treatment and modify the subsurface structure. Restricting elemental substitution to the near-surface region reduces the capacity loss associated with bulk doping of electrochemically inactive elements and also allows incorporation of cations that are hard to co-precipitate because of differences in solubility. In the studies presented here, single dopants were used, but investigations on the effect of two or more dopants on the near-surface region, as seen in bulk CAMs,[111,112] could be a future field of research. So far, studies combining the coating/doping strategy in Ni-rich CAMs mainly focused on oxides of Zr^{4+} ($r = 0.72$ Å), Al^{3+} ($r = 0.535$ Å), Mn^{4+} ($r = 0.53$ Å), Nb^{5+} ($r = 0.64$ Å), Mo^{6+} ($r = 0.59$ Å) and W^{6+} ($r = 0.6$ Å) (all r values for octahedral coordination).[113]

Zr-based surface doping was investigated in NCM811 by Schipper et al.[114] as well as in LNO by Cho et al.[115] and Yoon et al.[116] Zirconium was either introduced by deposition from zirconium alkoxides with a subsequent heat treatment[114,115] or by co-precipitation with the hydroxide reactant prior to the high-temperature lithiation.[116] The miscibility of Zr^{4+} is probably larger in LNO than in NCM, as indicated by lower onset temperature for dopant diffusion in the CAM (400 °C in LNO vs. 600 °C in NCM). Surface doping induced a lower interfacial charge transfer resistance of doped vs. undoped material, which could be attributed to surface layers of Li_2ZrO_3 in LNO[116] and ZrO_2[114] in NCM with thicknesses between 7 nm and 30 nm, as observed by TEM. Additionally, despite Zr being predominantly present in the subsurface region, Zr-doped LNO features a limited H2-to-H3 phase transition, thus mitigating the destructive effect of the volume contraction/expansion upon cycling. Overall, the capacity retention increased from 74 % to 86 % in LNO (2.7–4.3 V vs. Li^+/Li, C/2 rate) and 77 % to 88 % in NCM (2.7–4.3 V vs. Li^+/Li, C/5 rate, 30 °C).

In a similar study, 1 and 3 mol-% Mo-doped NCM811 were synthesized from the transition-metal nitrates, $(NH_4)_6Mo_7O_{24}\cdot 4H_2O$ and sucrose in a sol-gel process, then heated to self-ignition and calcined.[117] The individual primary particles were between 400 nm and 900 nm in the pristine material and 200–500 nm in the doped samples, indicating inhibition of particle growth by the dopant. DFT calculations suggest that the highly charged, small dopant is incorporated into the transition-metal layer and leads to a charge redistribution. TOF-SIMS and HAADF-STEM indicate that the Mo content is high at the surface and then decreases and levels off within the first 50 nm. Regarding cycling, the 1 mol-% Mo-doped sample represents the optimum with 148 mAh/g after 100 cycles (2.8– 4.3 V vs. Li^+/Li, C/3 rate, 30 °C) compared to 118 mAh/g for the pristine material. While the procedure does not yield a spherical morphology of secondary particles with controlled diameters and thus good long-term cycling data, the described process allows for fast screening of the effect of surface modifications.

Surface-modified, W-doped LNO and NCM have also been reported. The nickel hydroxide reactant was co-precipitated in the presence of WO_3 dissolved in NaOH, leading to an electrochemical optimum at 1 mol-% doping level.[3] During the high-temperature lithiation, tungsten migrates to the surface and/or grain boundaries and segregates into a W-doped rock salt-type

EurJIC
European Journal of Inorganic Chemistry

Minireview
doi.org/10.1002/ejic.202000408

Chemistry
Europe
European Chemical
Societies Publishing

LNO/NCM surface layer, as determined by TEM and DFT calculations. W-doped LNO delivers an initial specific capacity of 245 mAh/g. The cycling performance is also remarkably stable, showing a capacity retention of ca. 86 % after 100 cycles in the W-doped material (2.7–4.3 V vs. Li$^+$/Li, C/2 rate, 30 °C) vs. 74 % for the pristine LNO. Using the same testing conditions, W-doped NCM900505 (90 % Ni), NCM801505 (80 % Ni) and NC8911 (89 % Ni) exhibit excellent capacity retentions of ≥94 %, also confirmed by testing of full cells for 1000 cycles.

In a different approach, $Ni_{0.8}Mn_{0.1}Co_{0.1}(OH)_2$ was coated with $Al(OH)_3$ (or Al_2O_3) prior to lithiation, by combining the hydroxide with $NaAlO_2$ in aqueous conditions, followed by CO_2 treatment and a two-step high-temperature lithiation for doping levels of 1–5 wt.-%.[118] The authors observe a strong gradient of Al^{3+} within the first 1 μm via cross-sectional SEM-EDS as well as a 10 nm surface layer of a lithium aluminum oxide in TEM for the 3 wt.-%-doped sample. The surface-modified materials feature increased capacity retention of 99 % vs. 90 % for the pristine NCM811 (2.8–4.3 V vs. Li$^+$/Li, 1C rate), better capacity retention at higher upper cutoff voltages and improved performance at 5C rate (117 mAh/g vs. 37 mAh/g) in the sample doped with 1 wt.-%. However, no conclusions about the long-term performance can be drawn from this study, as cycling only proceeded to 60 cycles.

A different investigation focused on doping 1–5 mol-% Mn via an acetate coating on $Ni_{0.815}Co_{0.15}Al_{0.035}(OH)_2$ by wet chemistry.[119] The hydroxide was dehydrated at 450 °C, mixed with $LiOH·H_2O$ and fired again to 780 °C in O_2. The procedure results in a rock salt-like surface layer of thickness up to 25 nm for the 5 mol-% Mn sample, which contains mostly Ni^{2+}, Ni^{3+}, Co^{3+} and Mn^{4+}. According to TEM-EDS, the Mn content decreases strongly within the first 30 nm, which was confirmed by XPS experiments on pristine and etched samples. In the optimal case of 2 mol-% Mn, the surface layer increases the capacity retention to 91.3 % vs. 79.9 % for the pristine sample after 100 cycles (4.3 V cutoff, 1C rate).

Xin et al. created a Li-Nb-O surface layer on NCM811 via hydrolysis of Nb(V) ethoxide combined with subsequent firing to 500 °C.[120] The procedure induces diffusion of Nb^{5+} into the secondary particles and creates a gradient from about 4 at-% at the surface to below 1 at-% within the first 100 nm below the surface. In this work, the Nb^{5+} has been hypothesized to occupy the Li sites, which is in contrast to prior experiments on similar sized and charged Mo^{6+}, found primarily at the surface of NCM811.[117]

There is ambiguity on locating the dopant atoms in some of the presented studies. Classical X-ray methods used in bulk doping come to their detection limit because of the low dopant level, their confinement to the immediate subsurface region and constrained assignments of dopants to sites in the CAM lattice based on ionic radii. Unfortunately, there is rarely experimental proof for these hypotheses. Locating the dopant in surface-modified CAMs is challenging, as one needs to distinguish inclusion into the crystal lattice from the presence of intergranular films. Hence, it requires methods with either high spatial resolution and/or surface probing abilities, such as TEM, TOF-SIMS, XAS, XPS or HAXPES. These would help to further our understanding of the interaction between the dopant and the CAM (crystal structure, growth etc.), which in turn would improve our understanding of structure–property-relationships and the ability to stabilize interphases and interfaces.

4. Washing

Washing refers to the removal of surface contaminants of the CAM by a liquid. These contaminations are typically residual Li salts, such as LiOH, $LiOH·H_2O$ or Li_2CO_3, originating from the excess of Li-containing reactants, necessary to ensure a stoichiometric product, and subsequent storage in air.[121] Each of these residual lithium compounds is accompanied by undesired properties that become severe processing and safety issues during manufacturing and operation of LIBs. First, the basicity of the contaminants increases the pH value of the electrode slurry, which in combination with the hygroscopic nature of the common solvent used (N-methyl-2-pyrrolidon, NMP) results in gelation and thus processing issues. Second, the carbonate impurities evolve CO_2 during battery operation and were shown to be the main contributors to gassing in the first few cycles.[26,122,123] Third, both combined reduce the shelf life (storage under ambient conditions or in electrolyte) of Ni-rich CAMs significantly due to their own hygroscopy.[121,124] Accordingly, the removal of these surface impurities is crucial to improve storage and safety properties of Ni-rich NCMs and NCAs; however, the choice of solvent, the exposure duration and the subsequent drying conditions are of equal importance to the performance of such materials. The two main solvents used for the purpose of washing Ni-rich CAMs are water and ethanol.

4.1. Water-Based Washing and Processing

Washing using water as solvent is believed to not only remove impurities from the surface but also to modify the near-surface region through Li$^+$/H$^+$ exchange between the material and the washing solution.[1,27,125] As a consequence, water-processed materials (or materials stored under moist conditions) do not deliver the same specific charge/discharge capacities as pristine (unwashed) ones. They also distinctly differ in (de)lithiation behavior, evident in their respective voltage profiles, due to kinetic limitations induced by the loss of Li.[126] Nevertheless, water was established as the solvent of choice by most manufactures, which implies that this process can be optimized in terms of exposure duration and drying conditions to minimize the adverse effects of proton exchange.

In a recent paper, Pritzl et al.[27] investigated the underlying mechanism of washing and subsequent drying conditions of CAMs with a Ni content of 85 % with respect to battery performance. Their results indicate the presence of an oxygen-depleted rock salt-like surface layer related to the increase in drying temperature after washing. This presumably electrochemically inactive surface layer manifests itself in two ways: first, in the form of capacity loss because of the loss of Li (Figure 6a). Second, in the form of kinetic limitation that is evident from the polarization (overvoltage) and the prolonged constant voltage step of washed/high-temperature dried Ni-rich NCM

EurJIC
European Journal of Inorganic Chemistry

Minireview
doi.org/10.1002/ejic.202000408

Chemistry
Europe
European Chemical
Societies Publishing
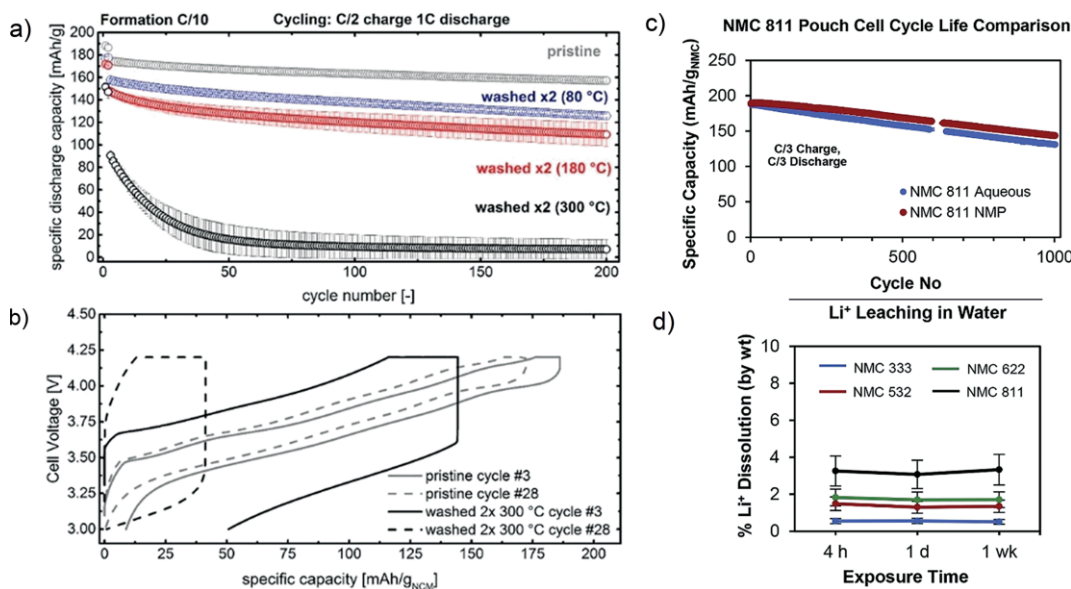
Figure 6. (a) Specific discharge capacities of the pristine NCM851005 cathode (not washed, dried at 120 °C, in gray), and of the washed NCM851005 cathodes dried at 80 °C (in blue), at 180 °C (in red), or at 300 °C (in black). (b) Full-cell voltage vs. capacity profiles of the 3rd and of the 28th cycle at C/2 charge and 1C discharge of the pristine NCM851005 cathode (in gray) and of the washed NCM851005 cathode dried at 300 °C. Reproduced from ref.[27] (c) Long-term cycling performance at C/3 rate of single-layer pouch cells with graphite anode and aqueous-processed NCM811 cathode and NMP-processed NCM811 cathode. (d) Lithium leached from high concentration NCM (ca. 63 wt.-%) into the filtrate for different NCM compositions in deionized water (pH 6.6). Reproduced from ref.[127]

(Figure 6b). Hence, this study highlights the compromise that has to be considered for Ni-rich CAMs.

As it appears, practical discharge capacity and cycle life have to be sacrificed to improve their safety and storage properties through a water-based washing process. However, it may still be possible to process Ni-rich materials in water, at least in the context of electrode preparation. Wood et al.[127] conducted a study on NCM811, comparing a traditional electrode slurry preparation process with a water-based process. Electrochemical properties of both processes were shown using single-layer pouch full cells under long-term cycling conditions. In contrast to previous reports,[128] their CAM shows no initial capacity loss and only minimal differences in capacity retention (4 % after 1000 cycles compared to the traditional NMP-based process) when exposed to water (Figure 6c). According to the authors, this behavior is based on an observation of Li+ leaching and its time dependency when NCM811 was exposed to water in a high water concentration (low solid content) or low water concentration (high solid content) environment. In other words, if water is present in excess, similar to a washing procedure, the amount of Li+ leached into the solution steadily increases over time. On the other hand, when water is scarce, as in a standard slurry preparation procedure (Figure 6d, only high solid concentration shown), the Li+ content remains constant even after one week of water exposure. This may indicate the possibility that protons present in the aqueous solution and involved in ion exchange can be limited to a degree such that the development of an electrochemically unstable surface layer is minimized. Unfortunately, the authors did not provide detailed surface analysis of the high solid content samples, which would allow for an assumption on the actual removal of any (residual) surface Li species. Hence, the question whether an aqueous

washing process that actively limits available water can produce impurity-free Ni-rich CAMs with pristine electrochemical properties remains unanswered.

4.2. Ethanol-Based Washing

Early investigations into washing effects on Ni-rich CAMs already suggested a different solvent, ethanol, to mitigate the drawbacks of water exposure.[124] However, from a manufacturer's perspective, ethanol is unlikely to be used due to the associated costs. Nevertheless, we will include this possibility for the sake of completeness. Based on these early findings, Zheng et al.[129] investigated ethanol as potential solvent to remove residual Li species with respect to electrochemical performance and long-term storage properties of NCM811. It was indeed demonstrated that ethanol does not lead to surface structural changes and corresponding deterioration of cycling performance, as expected. More significant, however, is the analysis of the improved long-term storage properties under ambient conditions. The authors claim that after storage for 40 days, NCM811 washed with ethanol shows much reduced reappearance of Li impurities (mainly Li_2CO_3) on the surface compared to the pristine material, because the absence of an ion exchange in the non-aqueous solvent leaves the near-surface structure intact, which was probed using TEM and XPS. It should be noted, nevertheless, that cycling data were only provided for 100 cycles and an evaluation of the long-term performance would be desirable. Furthermore, a detailed analysis on the gassing behavior to investigate a potential reduction of such could also be beneficial to evaluate the overall effect of an ethanol-based washing process.

EurJIC
European Journal of Inorganic Chemistry

Minireview
doi.org/10.1002/ejic.202000408

Chemistry Europe
European Chemical Societies Publishing

In light of these studies, a water-based sequential or simultaneous washing and slurry preparation process may become of profound importance for manufactures of Ni-rich CAMs. This is not only to improve the safety and storage properties of such materials but also as cost reduction opportunity by replacing NMP and polyvinylidene difluoride (PVDF) with more sustainable and cheaper alternatives. Similar approaches have already been investigated for less water-sensitive cathode and anode active materials, such as $LiFePO_4$, $LiCoO_2$ and graphite.[130]

5. Conclusion and Perspective

As shown in this minireview, various flavors of coatings, surface dopings and washing procedures are state of the art techniques to prolong the lifetime of Ni-rich NCM and NCA CAMs by increasing the interfacial stability. In the near future, the importance of surface modification strategies will grow, as the need for increasing Ni content limits dopant- and elemental gradient-based strategies. In addition, surface coatings play a crucial role in the functioning of all-solid-state batteries, representing a promising next-generation energy-storage technology. The reviewed literature suggests that a conformal and uniform coating is desirable to avoid O_2 evolution (and thus electrolyte oxidation) or HF attack, yet hard to achieve in practice.

The trend is moving from coverage by large nanoparticles to more dense films from small nanoparticles or from highly conformal, amorphous coatings via ALD or polymers. While many experiments aim at the very basic parameter of cycle number improvement, more fundamental experiments, for example, in non-classical electrochemical test setups,[131] would be desirable to investigate the influence of the degree of coverage, the coating material's real space structure or interactions between surface modifications and (surface) conductivity on the single particle level. These could also address the apparent paradox of improvement in rate capability upon the application of seemingly insulating coating or the fact that often surface reaction mechanisms are assumed, not proven. However, a combination of surface modifications with new avenues could interact synergistically, as for example in single-crystalline materials, where a conformal coating more efficiently engulfs the complete primary particle surface, compared to the currently used polycrystalline secondary particle structure.[40] Looking forward, we believe that surface modification and thus the studies reviewed here will play a major role in enabling the adoption of Ni-rich CAMs in real-world applications, paving the way for carbon-footprint reduction in energy-storage technologies.

[1] M. Bianchini, M. Roca-Ayats, P. Hartmann, T. Brezesinski, J. Janek, *Angew. Chem. Int. Ed.* **2019**, *58*, 10434–10458; *Angew. Chem.* **2019**, *131*, 10542–10569.
[2] C. Vaalma, D. Buchholz, M. Weil, S. Passerini, *Nat. Rev. Mater.* **2018**, *3*, 18013.
[3] U.-H. Kim, D.-W. Jun, K.-J. Park, Q. Zhang, P. Kaghazchi, D. Aurbach, D. T. Major, G. Goobes, M. Dixit, N. Leifer, C. M. Wang, P. Yan, D. Ahn, K.-H. Kim, C. S. Yoon, Y.-K. Sun, *Energy Environ. Sci.* **2018**, *11*, 1271–1279.
[4] G. Harper, R. Sommerville, E. Kendrick, L. Driscoll, P. Slater, R. Stolkin, A. Walton, P. Christensen, O. Heidrich, S. Lambert, A. Abbott, K. Ryder, L. Gaines, P. Anderson, *Nature* **2019**, *575*, 75–86.
[5] M. Ben Yahia, J. Vergnet, M. Saubanère, M.-L. Doublet, *Nat. Mater.* **2019**, *18*, 496–502.
[6] N. Li, S. Sallis, J. K. Papp, J. Wei, B. D. McCloskey, W. Yang, W. Tong, *ACS Energy Lett.* **2019**, *4*, 2836–2842.
[7] L. Liang, G. Hu, F. Jiang, Y. Cao, *J. Alloys Compd.* **2016**, *657*, 570–581.
[8] L. Liang, W. Zhang, F. Zhao, D. K. Denis, F. uz Zaman, L. Hou, C. Yuan, *Adv. Mater. Interfaces* **2020**, *7*, 1901749.
[9] A. O. Kondrakov, H. Geßwein, K. Galdina, L. de Biasi, V. Meded, E. O. Filatova, G. Schumacher, W. Wenzel, P. Hartmann, T. Brezesinski, J. Janek, *J. Phys. Chem. C* **2017**, *121*, 24381–24388.
[10] A. O. Kondrakov, A. Schmidt, J. Xu, H. Geßwein, R. Mönig, P. Hartmann, H. Sommer, T. Brezesinski, J. Janek, *J. Phys. Chem. C* **2017**, *121*, 3286–3294.
[11] S. Schweidler, L. de Biasi, G. Garcia, A. Mazilkin, P. Hartmann, T. Brezesinski, J. Janek, *ACS Appl. Energy Mater.* **2019**, *2*, 7375–7384.
[12] H.-H. Ryu, K.-J. Park, C. S. Yoon, Y.-K. Sun, *Chem. Mater.* **2018**, *30*, 1155–1163.
[13] S. Ahmed, A. Pokle, S. Schweidler, A. Beyer, M. Bianchini, F. Walther, A. Mazilkin, P. Hartmann, T. Brezesinski, J. Janek, K. Volz, *ACS Nano* **2019**, *13*, 10694–10704.
[14] H. Zhang, F. Omenya, P. Yan, L. Luo, M. S. Whittingham, C. Wang, G. Zhou, *ACS Energy Lett.* **2017**, *2*, 2607–2615.
[15] K. Ishizu, Y. Oka, T. Nakamura, *Solid State Ionics* **2016**, *288*, 176–179.
[16] L. de Biasi, A. O. Kondrakov, H. Geßwein, T. Brezesinski, P. Hartmann, J. Janek, *J. Phys. Chem. C* **2017**, *121*, 26163–26171.
[17] F. Strauss, L. de Biasi, A-Y. Kim, J. Hertle, S. Schweidler, J. Janek, P. Hartmann, T. Brezesinski, *ACS Materials Lett.* **2020**, *2*, 84–88.
[18] F. Kong, C. Liang, L. Wang, Y. Zheng, S. Perananthan, R. C. Longo, J. P. Ferraris, M. Kim, K. Cho, *Adv. Energy Mater.* **2019**, *9*, 1802586.
[19] J. Xu, F. Lin, M. M. Doeff, W. Tong, *J. Mater. Chem. A* **2017**, *5*, 874–901.
[20] A. T. S. Freiberg, M. K. Roos, J. Wandt, R. de Vivie-Riedle, H. A. Gasteiger, *J. Phys. Chem. A* **2018**, *122*, 8828–8839.
[21] L. de Biasi, A. Schiele, M. Roca-Ayats, G. Garcia, T. Brezesinski, P. Hartmann, J. Janek, *ChemSusChem* **2019**, *12*, 2240–2250.
[22] T. Bartsch, F. Strauss, T. Hatsukade, A. Schiele, A-Y. Kim, P. Hartmann, J. Janek, T. Brezesinski, *ACS Energy Lett.* **2018**, *3*, 2539–2543.
[23] J. Wandt, A. T. S. Freiberg, A. Ogrodnik, H. A. Gasteiger, *Mater. Today* **2018**, *21*, 825–833.
[24] T. M. Østergaard, L. Giordano, I. E. Castelli, F. Maglia, B. K. Antonopoulos, Y. Shao-Horn, J. Rossmeisl, *J. Phys. Chem. C* **2018**, *122*, 10442–10449.
[25] J. Paulsen, J. Kim, High Nickel Cathode Material Having Low Soluble Base Content, **2012**, US9698418B2.
[26] T. Hatsukade, A. Schiele, P. Hartmann, T. Brezesinski, J. Janek, *ACS Appl. Mater. Interfaces* **2018**, *10*, 38892–38899.
[27] D. Pritzl, T. Teufl, A. T. S. Freiberg, B. Strehle, J. Sicklinger, H. Sommer, P. Hartmann, H. A. Gasteiger, *J. Electrochem. Soc.* **2019**, *166*, A4056–A4066.
[28] J. Sicklinger, M. Metzger, H. Beyer, D. Pritzl, H. A. Gasteiger, *J. Electrochem. Soc.* **2019**, *166*, A2322–A2335.
[29] L. Hu, S. S. Zhang, Z. Zhang in *Rechargeable Batteries. Green Energy and Technology* (Eds.: Z. Zhang, S. Zhang), Springer, Cham, **2015**, pp. 231–261.
[30] D. R. Gallus, R. Schmitz, R. Wagner, B. Hoffmann, S. Nowak, I. Cekic-Laskovic, R. W. R. Schmitz, M. Winter, *Electrochim. Acta* **2014**, *134*, 393–398.
[31] J. Wandt, A. Freiberg, R. Thomas, Y. Gorlin, A. Siebel, R. Jung, H. A. Gasteiger, M. Tromp, *J. Mater. Chem. A* **2016**, *4*, 18300–18305.
[32] L. Wang, T. Maxisch, G. Ceder, *Chem. Mater.* **2007**, *19*, 543–552.
[33] T. Nakamura, K. Amezawa, J. Kulisch, W. G. Zeier, J. Janek, *ACS Appl. Mater. Interfaces* **2019**, *11*, 19968–19976.

EurJIC
European Journal of Inorganic Chemistry

Minireview
doi.org/10.1002/ejic.202000408

Chemistry
Europe
European Chemical
Societies Publishing

[34] J. Zheng, T. Liu, Z. Hu, Y. Wei, X. Song, Y. Ren, W. Wang, M. Rao, Y. Lin, Z. Chen, J. Lu, C. Wang, K. Amine, F. Pan, *J. Am. Chem. Soc.* **2016**, *138*, 13326–13334.

[35] M. D. Radin, S. Hy, M. Sina, C. Fang, H. Liu, J. Vinckeviciute, M. Zhang, M. S. Whittingham, Y. S. Meng, A. Van der Ven, *Adv. Energy Mater.* **2017**, *7*, 1602888.

[36] H.-J. Noh, S. Youn, C. S. Yoon, Y.-K. Sun, *J. Power Sources* **2013**, *233*, 121–130.

[37] J. Cabana, B. J. Kwon, L. Hu, *Acc. Chem. Res.* **2018**, *51*, 299–308.

[38] B. Xiao, X. Sun, *Adv. Energy Mater.* **2018**, *8*, 1802057.

[39] W. Yan, S. Yang, Y. Huang, Y. Yang, G. Yuan, *J. Alloys Compd.* **2020**, *819*, 153048.

[40] W. Lee, S. Muhammad, C. Sergey, H. Lee, J. Yoon, Y.-M. Kang, W.-S. Yoon, *Angew. Chem. Int. Ed.* **2020**, *59*, 2578–2605; *Angew. Chem.* **2020**, *132*, 2598–2626.

[41] P. Guan, L. Zhou, Z. Yu, Y. Sun, Y. Liu, F. Wu, Y. Jiang, D. Chu, *J. Energy Chem.* **2020**, *43*, 220–235.

[42] D. Aurbach, B. Markovsky, M. D. Levi, E. Levi, A. Schechter, M. Moshkovich, Y. Cohen, *J. Power Sources* **1999**, *81–82*, 95–111.

[43] K. Edström, T. Gustafsson, J. O. Thomas, *Electrochim. Acta* **2004**, *50*, 397–403.

[44] E. M. Erickson, W. Li, A. Dolocan, A. Manthiram, *ACS Appl. Mater. Interfaces* **2020**, *12*, 16451–16461.

[45] A. Jarry, S. Gottis, Y.-S. Yu, J. Roque-Rosell, C. Kim, J. Cabana, J. Kerr, R. Kostecki, *J. Am. Chem. Soc.* **2015**, *137*, 3533–3539.

[46] D. Becker, M. Börner, R. Nölle, M. Diehl, S. Klein, U. Rodehorst, R. Schmuch, M. Winter, T. Placke, *ACS Appl. Mater. Interfaces* **2019**, *11*, 18404–18414.

[47] J.-c. Zheng, Z. Yang, Z.-j. He, H. Tong, W.-j. Yu, J.-f. Zhang, *Nano Energy* **2018**, *53*, 613–621.

[48] Y.-D. Xu, W. Xiang, Z.-G. Wu, C.-L. Xu, Y.-C. Li, X.-D. Guo, G.-P. Lv, X. Peng, B.-H. Zhong, *Electrochim. Acta* **2018**, *268*, 358–365.

[49] S. Ito, S. Fujiki, T. Yamada, Y. Aihara, Y. Park, T. Y. Kim, S.-W. Baek, J.-M. Lee, S. Doo, N. Machida, *J. Power Sources* **2014**, *248*, 943–950.

[50] R. Jung, M. Metzger, F. Maglia, C. Stinner, H. A. Gasteiger, *J. Electrochem. Soc.* **2017**, *164*, A1361–A1377.

[51] S. F. Lux, I. T. Lucas, E. Pollak, S. Passerini, M. Winter, R. Kostecki, *Electrochem. Commun.* **2012**, *14*, 47–50.

[52] M. Aykol, S. Kirklin, C. Wolverton, *Adv. Energy Mater.* **2014**, *4*, 1400690.

[53] M. Aykol, S. Kim, V. I. Hegde, D. Snydacker, Z. Lu, S. Hao, S. Kirklin, D. Morgan, C. Wolverton, *Nat. Commun.* **2016**, *7*, 13779.

[54] K. Du, H. Xie, G. Hu, Z. Peng, Y. Cao, F. Yu, *ACS Appl. Mater. Interfaces* **2016**, *8*, 17713–17720.

[55] Y. Zhao, Z. Lv, T. Xu, J. Li, *J. Alloys Compd.* **2017**, *715*, 105–111.

[56] Y.-K. Sun, Y.-S. Lee, M. Yoshio, K. Amine, *Electrochem. Solid-State Lett.* **2002**, *5*, A99–A102.

[57] Z. Gan, G. Hu, Z. Peng, Y. Cao, H. Tong, K. Du, *Appl. Surf. Sci.* **2019**, *481*, 1228–1238.

[58] J. Duan, C. Wu, Y. Cao, K. Du, Z. Peng, G. Hu, *Electrochim. Acta* **2016**, *221*, 14–22.

[59] S. N. Lim, W. Ahn, S.-H. Yeon, S. Bin Park, *Electrochim. Acta* **2014**, *136*, 1–9.

[60] S. H. Jang, K.-J. Lee, J. Mun, Y.-K. Han, T. Yim, *J. Power Sources* **2019**, *410–411*, 15–24.

[61] M.-T. F. Rodrigues, C. Liao, K. Kalaga, I. A. Shkrob, D. P. Abraham, *ACS Appl. Energy Mater.* **2019**, *2*, 5380–5385.

[62] K. Park, J.-H. Park, S.-G. Hong, B. Choi, S.-W. Seo, J.-H. Park, K. Min, *Phys. Chem. Chem. Phys.* **2016**, *18*, 29076–29085.

[63] J. Zhang, J. Zhang, X. Ou, C. Wang, C. Peng, B. Zhang, *ACS Appl. Mater. Interfaces* **2019**, *11*, 15507–15516.

[64] K. Heo, J.-S. Lee, H.-S. Kim, M.-Y. Kim, H. Jeong, J. Kim, J. Lim, *J. Electrochem. Soc.* **2018**, *165*, A2955–A2960.

[65] S. Chen, T. He, Y. Su, Y. Lu, L. Bao, L. Chen, Q. Zhang, J. Wang, R. Chen, F. Wu, *ACS Appl. Mater. Interfaces* **2017**, *9*, 29732–29743.

[66] Q. Gan, N. Qin, Y. Zhu, Z. Huang, F. Zhang, S. Gu, J. Xie, K. Zhang, L. Lu, Z. Lu, *ACS Appl. Mater. Interfaces* **2019**, *11*, 12594–12604.

[67] Y. J. Kim, J. Cho, T.-J. Kim, B. Park, *J. Electrochem. Soc.* **2003**, *150*, A1723–A1725.

[68] S. Hildebrand, C. Vollmer, M. Winter, F. M. Schappacher, *J. Electrochem. Soc.* **2017**, *164*, A2190–A2198.

[69] G. Wu, Y. Zhou, *J. Energy Chem.* **2019**, *28*, 151–159.

[70] J. Xiang, C. Chang, L. Yuan, J. Sun, *Electrochem. Commun.* **2008**, *10*, 1360–1363.

[71] S. Neudeck, A. Mazilkin, C. Reitz, P. Hartmann, J. Janek, T. Brezesinski, *Sci. Rep.* **2019**, *9*, 5328.

[72] S. Neudeck, F. Strauss, G. Garcia, H. Wolf, J. Janek, P. Hartmann, T. Brezesinski, *Chem. Commun.* **2019**, *55*, 2174–2177.

[73] Y. Cho, Y.-S. Lee, S.-A. Park, Y. Lee, J. Cho, *Electrochim. Acta* **2010**, *56*, 333–339.

[74] Y. Xu, X. Li, Z. Wang, H. Guo, B. Huang, *Mater. Lett.* **2015**, *143*, 151–154.

[75] S. M. Lee, S. H. Oh, J. P. Ahn, W. I. Cho, H. Jang, *J. Power Sources* **2006**, *159*, 1334–1339.

[76] W. Liu, G. Hu, K. Du, Z. Peng, Y. Cao, *Surf. Coat. Technol.* **2013**, *216*, 267–272.

[77] X. He, C. Du, B. Shen, C. Chen, X. Xu, Y. Wang, P. Zuo, Y. Ma, X. Cheng, G. Yin, *Electrochim. Acta* **2017**, *236*, 273–279.

[78] X. Xiong, D. Ding, Y. Bu, Z. Wang, B. Huang, H. Guo, X. Li, *J. Mater. Chem. A* **2014**, *2*, 11691–11696.

[79] Z.-F. Tang, R. Wu, P.-F. Huang, Q.-S. Wang, C.-H. Chen, *J. Alloys Compd.* **2017**, *693*, 1157–1163.

[80] Y. Zeng, J. He, *J. Power Sources* **2009**, *189*, 519–521.

[81] B. Huang, X. Li, Z. Wang, H. Guo, *Mater. Lett.* **2014**, *131*, 210–213.

[82] K. Min, K. Park, S. Y. Park, S.-W. Seo, B. Choi, E. Cho, *Sci. Rep.* **2017**, *7*, 7151.

[83] H.-B. Kim, B.-C. Park, S.-T. Myung, K. Amine, J. Prakash, Y.-K. Sun, *J. Power Sources* **2008**, *179*, 347–350.

[84] S.-H. Lee, C. S. Yoon, K. Amine, Y.-K. Sun, *J. Power Sources* **2013**, *234*, 201–207.

[85] X. Xiong, Z. Wang, X. Yin, H. Guo, X. Li, *Mater. Lett.* **2013**, *110*, 4–9.

[86] J. Xie, A. D. Sendek, E. D. Cubuk, X. Zhang, Z. Lu, Y. Gong, T. Wu, F. Shi, W. Liu, E. J. Reed, Y. Cui, *ACS Nano* **2017**, *11*, 7019–7027.

[87] W. Liu, X. Tang, M. Qin, G. Li, J. Deng, X. Huang, *Mater. Lett.* **2016**, *185*, 96–99.

[88] S. W. Doo, S. Lee, H. Kim, J. H. Choi, K. T. Lee, *ACS Appl. Energy Mater.* **2019**, *2*, 6246–6253.

[89] B. G. Rao, D. Mukherjee, B. M. Reddy in *Nanostructures for Novel Therapy* (Eds.: D. Ficai, A. Grumezescu), Elsevier, **2017**, pp. 1–36.

[90] G. W. Scherer in *Encyclopedia of Materials: Science and Technology* (Eds.: K. H. J. Buschow, R. W. Cahn, M. C. Flemings, B. Ilschner, E. J. Kramer, S. Mahajan, P. Veyssière), Elsevier, **2001**, pp. 9797–9799.

[91] J. G. Speight in *Reaction Mechanisms in Environmental Engineering*, Elsevier, **2018**, pp. 337–384.

[92] P. Liu, L. Xiao, Y. Chen, H. Chen, *Ceram. Int.* **2019**, *45*, 18398–18405.

[93] F. Xiong, Z. Chen, C. Huang, T. Wang, W. Zhang, Z. Yang, F. Chen, *Inorg. Chem.* **2019**, *58*, 15498–15506.

[94] S. Dembski, C. Schneider, B. Christ, M. Retter in *Core-Shell Nanostructures for Drug Delivery and Theranostics* (Eds.: M. L. Focarete, A. Tampieri), Elsevier, **2018**, pp. 119–141.

[95] A. Shrivastava in *Introduction to Plastics Engineering*, Elsevier, **2018**, pp. 17–48.

[96] H. M. C. De Azeredo, M. F. Rosa, M. De Sá, M. Souza Filho, K. W. Waldron in *Advances in Biorefineries* (Ed.: K. W. Waldron), Elsevier, **2014**, pp. 819–874.

[97] Y. Cao, X. Qi, K. Hu, Y. Wang, Z. Gan, Y. Li, G. Hu, Z. Peng, K. Du, *ACS Appl. Mater. Interfaces* **2018**, *10*, 18270–18280.

[98] S. M. George, *Chem. Rev.* **2010**, *110*, 111–131.

[99] D. Mohanty, K. Dahlberg, D. M. King, L. A. David, A. S. Sefat, D. L. Wood, C. Daniel, S. Dhar, V. Mahajan, M. Lee, F. Albano, *Sci. Rep.* **2016**, *6*, 26532.

[100] L. David, K. Dahlberg, D. Mohanty, R. E. Ruther, A. Huq, M. Chi, S. J. An, C. Mao, D. M. King, L. Stevenson, D. L. Wood, *ACS Appl. Energy Mater.* **2019**, *2*, 1308–1313.

[101] W. Zhu, X. Huang, T. Liu, Z. Xie, Y. Wang, K. Tian, L. Bu, H. Wang, L. Gao, J. Zhao, *Coatings* **2019**, *9*, 92.

[102] O. Srur-Lavi, V. Miikkulainen, B. Markovsky, J. Grinblat, M. Talianker, Y. Fleger, G. Cohen-Taguri, A. Mor, Y. Tal-Yosef, D. Aurbach, *J. Electrochem. Soc.* **2017**, *164*, A3266–A3275.

[103] X. Cheng, J. Zheng, J. Lu, Y. Li, P. Yan, Y. Zhang, *Nano Energy* **2019**, *62*, 30–37.

EurJIC
European Journal of Inorganic Chemistry

Minireview
doi.org/10.1002/ejic.202000408

Chemistry
Europe
European Chemical
Societies Publishing

[104] W. M. M. Kessels, "Database of ALD processes", DOI: https://doi.org/10.6100/alddatabase can be found under https://www.atomiclimits.com/alddatabase/, **2019**.

[105] H. Maleki Kheimeh Sari, X. Li, *Adv. Energy Mater.* **2019**, *9*, 1901597.

[106] P. Poodt, D. C. Cameron, E. Dickey, S. M. George, V. Kuznetsov, G. N. Parsons, F. Roozeboom, G. Sundaram, A. Vermeer, *J. Vac. Sci. Technol. A* **2012**, *30*, 010802.

[107] R. S. Negi, S. P. Culver, A. Mazilkin, T. Brezesinski, M. T. Elm, *ACS Appl. Mater. Interfaces* **2020**, *12*, 31392–31400.

[108] G. D. Park, Y. Chan Kang, *RSC Adv.* **2014**, *4*, 44203–44207.

[109] C. Delmas, L. Croguennec, *MRS Bull.* **2002**, *27*, 608–612.

[110] Y. P. Wu, E. Rahm, R. Holze, *Electrochim. Acta* **2002**, *47*, 3491–3507.

[111] L. Mu, R. Zhang, W. H. Kan, Y. Zhang, L. Li, C. Kuai, B. Zydlewski, M. M. Rahman, C.-J. Sun, S. Sainio, M. Avdeev, D. Nordlund, H. L. Xin, F. Lin, *Chem. Mater.* **2019**, *31*, 9769–9776.

[112] L. Mu, W. H. Kan, C. Kuai, Z. Yang, L. Li, C.-J. Sun, S. Sainio, M. Avdeev, D. Nordlund, F. Lin, *ACS Appl. Mater. Interfaces* **2020**, *12*, 12874–12882.

[113] R. D. Shannon, *Acta Crystallogr., Sect. A* **1976**, *32*, 751–767.

[114] F. Schipper, H. Bouzaglo, M. Dixit, E. M. Erickson, T. Weigel, M. Talianker, J. Grinblat, L. Burstein, M. Schmidt, J. Lampert, C. Erk, B. Markovsky, D. T. Major, D. Aurbach, *Adv. Energy Mater.* **2018**, *8*, 1701682.

[115] J. Cho, T.-J. Kim, Y. J. Kim, B. Park, *Electrochem. Solid-State Lett.* **2001**, *4*, A159–A162.

[116] C. S. Yoon, U.-H. Kim, G.-T. Park, S. J. Kim, K.-H. Kim, J. Kim, Y.-K. Sun, *ACS Energy Lett.* **2018**, *3*, 1634–1639.

[117] F. A. Susai, D. Kovacheva, A. Chakraborty, T. Kravchuk, R. Ravikumar, M. Talianker, J. Grinblat, L. Burstein, Y. Kauffmann, D. T. Major, B. Markovsky, D. Aurbach, *ACS Appl. Energy Mater.* **2019**, *2*, 4521–4534.

[118] M. Dong, Z. Wang, H. Li, H. Guo, X. Li, K. Shih, J. Wang, *ACS Sustain. Chem. Eng.* **2017**, *5*, 10199–10205.

[119] C.-L. Xu, W. Xiang, Z.-G. Wu, Y.-D. Xu, Y.-C. Li, M.-Z. Chen, G. XiaoDong, G.-P. Lv, J. Zhang, B.-H. Zhong, *ACS Appl. Mater. Interfaces* **2018**, *10*, 27821–27830.

[120] F. Xin, H. Zhou, X. Chen, M. Zuba, N. Chernova, G. Zhou, M. S. Whittingham, *ACS Appl. Mater. Interfaces* **2019**, *11*, 34889–34894.

[121] J. Kim, H. Lee, H. Cha, M. Yoon, M. Park, J. Cho, *Adv. Energy Mater.* **2018**, *8*, 1702028.

[122] R. Robert, C. Bünzli, E. J. Berg, P. Novák, *Chem. Mater.* **2015**, *27*, 526–536.

[123] S. E. Renfrew, B. D. McCloskey, *J. Am. Chem. Soc.* **2017**, *139*, 17853–17860.

[124] R. Moshtev, P. Zlatilova, S. Vasilev, I. Bakalova, A. Kozawa, *J. Power Sources* **1999**, *81–82*, 434–441.

[125] N. V. Faenza, L. Bruce, Z. W. Lebens-Higgins, I. Plitz, N. Pereira, L. F. J. Piper, G. G. Amatucci, *J. Electrochem. Soc.* **2017**, *164*, A3727–A3741.

[126] I. A. Shkrob, J. A. Gilbert, P. J. Phillips, R. Klie, R. T. Haasch, J. Bareño, D. P. Abraham, *J. Electrochem. Soc.* **2017**, *164*, A1489–A1498.

[127] M. Wood, J. Li, R. E. Ruther, Z. Du, E. C. Self, H. M. Meyer, C. Daniel, I. Belharouak, D. L. Wood, *Energy Storage Mater.* **2020**, *24*, 188–197.

[128] N. Loeffler, G.-T. Kim, F. Mueller, T. Diemant, J.-K. Kim, R. J. Behm, S. Passerini, *ChemSusChem* **2016**, *9*, 1112–1117.

[129] X. Zheng, X. Li, Z. Wang, H. Guo, Z. Huang, G. Yan, D. Wang, *Electrochim. Acta* **2016**, *191*, 832–840.

[130] W. B. Hawley, J. Li, *J. Energy Storage* **2019**, *25*, 100862.

[131] S. Burkhardt, M. S. Friedrich, J. K. Eckhardt, A. C. Wagner, N. Bohn, J. R. Binder, L. Chen, M. T. Elm, J. Janek, P. J. Klar, *ACS Energy Lett.* **2019**, *4*, 2117–2123.